

LASER-INDUCED FLUORESCENCE STUDY ON THE QUENCHING RATES OF ELECTRONICALLY EXCITED SULFUR DIOXIDE WITH ALCHOLS

Yoshinori MURAKAMI¹, Katsuhiko SUZUKI², Yusuke ASAKAWA²
and Nobuyuki FUJII²

¹Department of Materials Engineering, Nagaoka National College of Technology

²Department of Chemistry, Nagaoka University of Technology

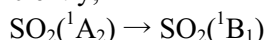
The relaxation kinetics for the electronically excited $\text{SO}_2(^1\text{A}_2)$ was investigated by measuring the time profiles for the laser-induced fluorescence intensities after the excitation of Clements F band of SO_2 molecules at around 303 nm. The semi-log plots for these time profiles were bent at $150 \mu\text{s}$ after the UV-laser excitations and thus co-existence of the fast and slow relaxation mechanisms was suggested for the relaxation of the electronically excited $\text{SO}_2(^1\text{A}_2)$. The quenching rate constants of the electronically excited $\text{SO}_2(^1\text{A}_2)$ with several kinds of alcohols were also investigated and it was found that the collisional quenching cross sections σ_q were well correlated with the well-depth ε of the interactions between the bath gases.

Key Words: laser-induced fluorescence, quenching, sulfur dioxide, alcohol

1. INTRODUCTION

Since sulfur dioxide (SO_2) is known as one of the most widely recognized atmospheric pollutants, a number of authors have investigated the reactions of SO_2 in air. Although the photochemical reactions between the electronically excited SO_2 and hydrocarbons are known to produce the unvolatile products,^{1), 2)} the reaction mechanism was complex and still remained unclear. This is partly due to the complicated interactions among the excited states of SO_2 as well as the unresolved relaxation kinetics of the electronically excited SO_2 formed by the UV light illuminations.

Fig. 1 is the schematic diagram of the electronic structures of SO_2 . As shown in **Fig. 1**, the $^1\text{A}_2$ state, the $^1\text{B}_1$ state and the $^3\text{B}_1$ state overlap with each other. Especially the vibronic couplings between the $^1\text{A}_2$ state and $^1\text{B}_1$ state are so strong that the internal conversions from $^1\text{A}_2$ level to $^1\text{B}_1$ level occurred very efficiently,



followed by the subsequent relaxations from the $^1\text{B}_1$ state to the $^3\text{B}_1$ state via the intersystem crossings. Furthermore the relaxation processes from the $^1\text{A}_2$ state to the $^1\text{A}_1$ ground state also occurred simultaneously via the resonant or non-resonant fluorescence.³⁾

In the presence of the hydrocarbons these quenching

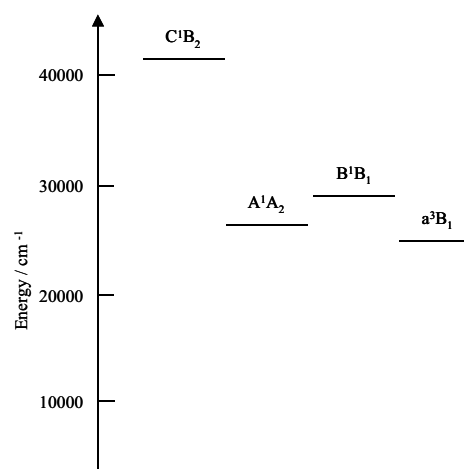


Fig. 1 Energy diagrams for the ground and excited states of SO_2 .

ng processes were influenced by collisional quenching between the electronically excited SO_2 with hydrocarbons and therefore the detailed understanding of such quenching processes is very important.

In the present work we have attempted to monitor the relaxation kinetics after the UV-excitation of SO_2 using the laser-induced fluorescence technique and to find the relationships between the collisional quenching cross sections and molecular properties.

2. EXPERIMENTAL

The arrangement of the experimental setup have been described elsewhere.⁴⁾ Briefly, the glass cell was evacuated up to 10^{-4} Torr before the experiment and then filled with about 1 Torr of SO_2 . For the quenching measurements the mixed gas of alcohol/ SO_2 were introduced in the glass cell and flowed slowly to avoid contaminations inside the glass cell.

The probe laser, which was generated by the frequency doubling of the dye laser pumped by the Nd:YAG laser, was irradiated to the glass cell and the fluorescence was collected by the photomultiplier tube which was placed perpendicular to the probe laser beam. The time-resolved fluorescence decays were monitored by the digitizing oscilloscope with the averaging of about 3000 measurements.

3. RESULTS AND DISCUSSIONS

Fig. 2 shows a typical example for the laser-induced fluorescence (LIF) spectra obtained when 1 Torr of SO_2 was filled in the glass cell. As shown in **Fig. 2**, the Clements E, F and G bands of SO_2 were observed as the fluorescence peaks.⁵⁾ By fixing the wavelength of the dye laser at the Clements F band, the time profiles for the laser-induced fluorescence intensities were measured. Typical examples of the fluorescence decays and the semilog plots were given in **Fig. 3(a)** and **Fig. 3(b)**. As shown in **Fig. 3(b)** the semi-log plot of the SO_2 LIF intensities was bent at around $150 \mu\text{s}$ and therefore they had two decay components, indicating that the radiative decay process for the electronically excited SO_2 was not a single process.

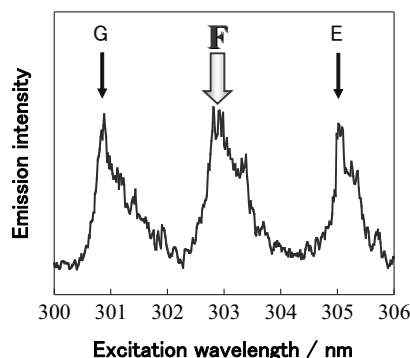


Fig. 2 Laser-induced fluorescence spectra of SO_2 .

To confirm such multiple decay processes for the SO_2 -LIF intensities, we have measured the time profiles of the dispersed fluorescence through a monochromator. For these measurements the excitation wavelength was changed from that of the Clements F band to 266 nm, which was generated by

the 4th harmonic of Nd:YAG laser. The semilog plots for the dispersed fluorescence of SO_2 were given in **Fig. 4**. When the wavelength of the fluorescence detection became longer than 350 nm, the semilog plots of the fluorescence decays was almost straight, but the wavelength of the fluorescence detection became as short as 280 nm, the bent structures for the semilog plots of the fluorescence intensities became prominent (see **Fig. 4**). This could be explained when the dispersed fluorescence longer than 350 nm was originated only from $^1\text{A}_2$ state, but the dispersed fluorescence observed at 280 nm was combination of the fluorescence for the pure $^1\text{A}_2$ state and for the mixed

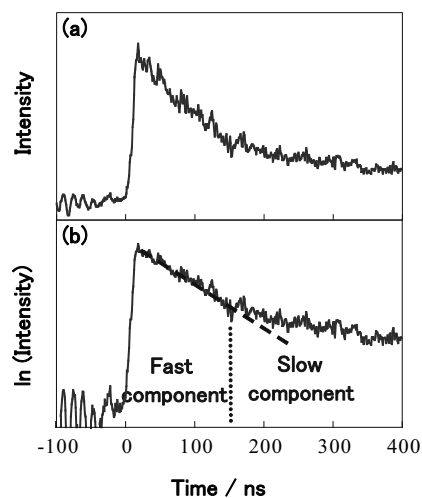


Fig. 3 A typical examples for the time profiles and semilog plots of SO_2 -LIF intensities.

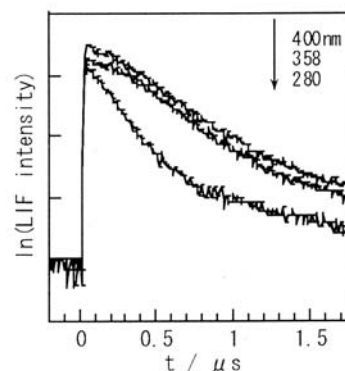


Fig. 4 Semilog plots of the dispersed fluorescence of SO_2 with excitation of 266 nm laser light.

states of the $^1\text{A}_2$ and $^1\text{B}_1$ states. This is consistent with the energy diagram of **Fig. 1** that shows the energy level of the $^1\text{B}_1$ state is higher than that of the $^1\text{A}_2$ state.

Bae et al.⁶⁾ also investigated the relaxation kinetics on the first singlet excited state of SO_2 from the time-resolved fluorescence intensities in the 300-450

nm region. They found the semi-log plot of time profiles of the SO₂ LIF intensities had fast and slow decay components. They further analyzed the time resolved emission spectra with different delay times. They found many sharp fluorescence peaks appeared just after the excitation of SO₂ and then broad continuum emission appeared at 100 - 300 ns after the excitation of SO₂. Finally the phosphorescence between 400-450 nm appeared after 1 μs of the excitation. They assigned the sharp fluorescence peaks and the broad continuum as the ¹A₁ state and the strong mixing state of ¹A₁ and ¹B₁, respectively. Their conclusions are consistent with our previous conclusions. Thus the different decay rates observed in **Fig. 2(b)** were probably due to the different radiative lifetimes for these excited states between the ¹A₁ and the mixing state of ¹A₁ and ¹B₁.

Next we have tried to measure the quenching rate constants for these excited states by adding several

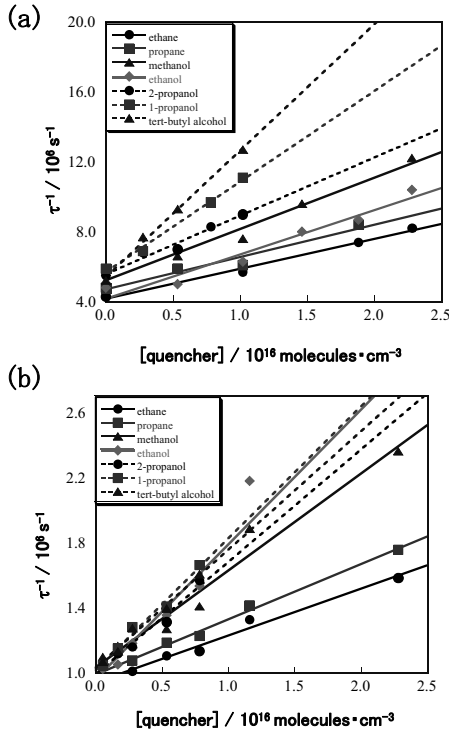


Fig. 5 Stern-Volmer plot for the decay rates of SO₂ fluorescence. (a) Faster component and (b) slower component. ●(solid line): ethane, ■(solid line): propane, ▲(solid line): methanol, ◆(solid line): ethanol, ●(dashed line): 2-propanol, ■(dashed line): 1-propanol, ▲(dashed line): t-butyl alcohol.

kinds of alcohols. **Fig. 5(a)** and **Fig. 5(b)** shows the Stern-Volmer plot for the fast and slower components of the SO₂ LIF decays. As seen in these figures, relatively good linearities were obtained. By

Table 1. Quenching rate constants and quenching cross sections for fast and slow components

quencher	Fast component		Slow component	
	k _q ^{*)}	σ _q ^{**)}	k _q ^{*)}	σ _q ^{**)}
ethane	1.72	3.09	1.32	2.37
propane	1.85	3.76	1.76	3.58
methanol	2.94	5.40	3.30	6.07
ethanol	2.54	5.23	4.27	8.79
2-propanol	3.34	7.40	3.76	8.33
1-propanol	5.18	11.47	4.67	10.34
tert-butyl alcohol	7.23	16.86	4.35	10.14

^{*)} 10⁻¹⁰cm³ · molecule⁻¹

^{**)} 10⁻¹⁵cm²

fitting these decay profiles with linear regressions, the quenching rate constant of SO₂ with alcohol for each of the fast and slow components was obtained.

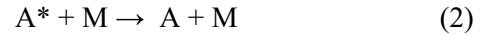
The results were summarized in **Table 1**. Since the quenching rate constant is dependent of the colliding velocities, the quenching rate constants k_q were converted to the quenching cross section σ_q via the following equation

$$\sigma_q = k_q / v \quad (1)$$

where v is the thermal velocity of colliding gases.

As you can see in **Table 1**, the quenching cross section became larger when the size of alcohols became larger. Since Parmenter and co-workers⁷⁾ have found the correlations between the quenching cross section σ_q and well-depth ε for the interactions between the electronically excited molecules and the quenching gas, we have attempted to adopt their theory to our experimental results.

According to their previous reports in Ref. 7, for the reaction of



where A* is the electronically excited species and M is the molecules or atoms that quench A*. For such reaction the quenching cross section σ_q can be expressed as follows,

$$\sigma_q = C \exp(\epsilon_{A^*M} / kT) \quad (3)$$

where k and T are the Boltzmann constant and the temperature, respectively. ε_{A*_M} is the well-depth for the interactions between A* and M. C is a constant obtained with empirical fit to the experimental expressed as the combination relationship values. Assuming the well-depth ε_{A*_M} can be ε_{A*_M}=(ε_{A*_{A*}}

$\epsilon_{A^*M})^{1/2}$, the above equation can be transformed to become

$$\ln(\sigma_q) = \ln(C) + \beta (\epsilon_{MM} / k)^{1/2} \quad (4)$$

where $\beta = (\epsilon_{A^*A^*} / kT^2)^{1/2}$ and ϵ_{MM} is the well-depth for the interactions between M themselves. Thus the plots for the logarithm of σ_q versus $(\epsilon_{MM} / kT^2)^{1/2}$ should be linear. Since the well-depths ϵ_{MM} are often not available for a substantial number of gases, therefore we have adopted the following empirical rules

$$\epsilon_{MM} / k \approx 1.5 T_b \quad (5)$$

where T_b is the boiling point of gases in K.⁸⁾

The results of the plots for the logarithm of σ_q versus $(\epsilon_{MM} / kT^2)^{1/2}$ in the present SO₂/alcohol system are shown in Fig. 6.

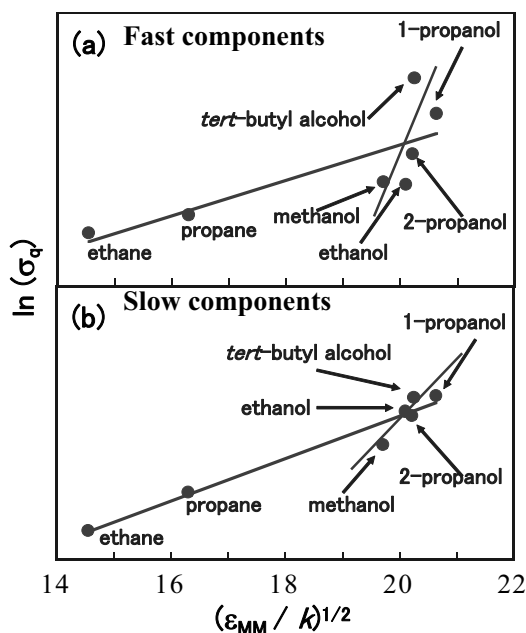


Fig. 6 The semilog plots for the quenching cross sections σ_q versus $(\epsilon_{MM} / kT^2)^{1/2}$ in the present SO₂/alcohol system

As shown in Fig. 6, good correlations were obtained in the the plots for the logarithm of σ_q versus $(\epsilon_{MM} / kT^2)^{1/2}$ in the present SO₂/alcohol system (both for (a) fast and (b) slow components). However the slope in the present SO₂/alcohol systems was two time higher than those of the SO₂/alkane system. The reason is not clear, but such difference might suggest some possibilities that alcohol/SO₂ system has different quenching mechanism because of the existence of hydrogen bondings between alcohols. Including the accurate measurements of the well-depth ϵ_{MM} , further

work is still needed for clarifying the differences.

4. CONCLUSIONS

Temporal decays for the SO₂-LIF intensities were found to have fast and slow components. Based on the dispersed fluorescence analysis, it was suggested that the fast component was the fluorescence from ¹A₂ and the slower component was that from the mixing state of ¹A₂ and ¹B₁ states.

The quenching cross sections of the electronically excited SO₂ with alcohols were measured and it was found that the good linear relationships were obtained in the the plots for the logarithm of σ_q versus $(\epsilon_{MM} / kT^2)^{1/2}$. However the slope of the plots for $\ln(\sigma_q)$ versus $(\epsilon_{MM} / kT^2)^{1/2}$ in the SO₂/alcohol system was about two times higher than that in the SO₂/alkane system and therefore the roles of the hydrogen bondings to the quenching processes in the SO₂/alcohol system was suggested.

REFERENCES

- 1) C.C.Badcock, H.W.Sidebottom, J.G.Calvert, G.W.Reinhardt and E.K. Damon, *Mechanism of the Photolysis of Sulfur Dioxide-Paraffin Hydrocarbon Mixtures*. J.Am.Chem.Soc. **93**, pp.3115-3121, 1971.
- 2) H.W.Sidebottom, C.C. Badcock, J.G. Calvert, B.R.Rabe and E.K. Damon : *Mechanism of the Photolysis of Mixtures of Sulfur Dioxide with Olefin and Aromatic Hydrocarbons*. J.Am.Chem.Soc. **93**, pp. 3115-3121, 1971.
- 3) E.Hegazi, F.Al-Adel, A. Hamdan, A. Dastageer, *Fluorescence of Indirectly Excited Low Vibrational Levels of the ¹A₂ State of Sulfur Dioxide*. J. Phys. Chem. **98**, pp.12169-12175, 1994.
- 4) Y.Murakami, Y.Sugatani and Y.Nosaka, *Laser- induced Incandescence study on the metal aerosol particles as the effect of the surrounding gas medium*. J.Phys.Chem.A. **109**, pp.8994-9000, 2005.
- 5) J.H.Clements, *On the absorption Spectrum of Sulfur Dioxide*. Physical Review. **47**, pp.224-232, 1934.
- 6) S.C.Bae, G.H.Kim and J.K.Ku, *Relaxation Kinetics on the First Excited Singlet State of SO₂ from Time Resolved Emission Spectra*, Chem. Phys. Lett. **265**, pp. 385-391, 1997.
- 7) M.H.Lin, M.Seaver, K.Y.Tang, A.E.W.Knight and C.S. Parmenter, *The roles of intermolecular potential well depths in collision-induced state change*. J. Chem. Phys. **70**, pp.5442-5457.
- 8) J.O.Herschfelder, C.F.Curtiss and R.F.Bird, *Molecular Theory of Liquids and Gases*, Wiley, New York, 1954.

(Received September 29, 2010)